

## A diabatic generalization of the quasigeostrophic frontogenesis function

M. Y. LUNA, M. L. MARTÍN, J. DE LA CRUZ and F. VALERO

*Dpto. Astrofísica y CC. de la Atmósfera, Facultad de CC. Físicas,  
Universidad Complutense de Madrid, 28040 Madrid, Spain.*

(Manuscript received Oct. 30, 2000; accepted in final form Jan. 16, 2001)

### RESUMEN

Una generalización de la función frontogenética es definida mediante la temperatura potencial del agua líquida-hielo, variable termodinámica conservativa en todos los cambios de fase del agua. La función frontogenética generalizada es la proyección de un nuevo vector,  $Q^*$ , sobre el gradiente de temperatura potencial del agua líquida-hielo.  $Q^*$  puede entenderse como la versión adiabática del vector quasigeostrofico  $Q$ . En zonas con liberación de calor latente debido a cambios de fase, la función frontogenética generalizada,  $F^*$ , resulta ser una herramienta más precisa y completa que la función frontogenética quasigeostrofica clásica para delimitar flujos de aire ascendente en zonas frontales. La función frontogenética propuesta es validada en una situación meteorológica real caracterizada por la creación y el desarrollo de un frente cálido sobre el norte de la Península Ibérica. Se compara con la función clásica de Pettersen comprobando que la función frontogenética generalizada no sólo diagnostica mejor los desarrollos frontales sino que además sitúa con mayor exactitud la posición de las zonas frontales.

### ABSTRACT

A generalized frontogenesis function is defined in terms of the ice-liquid water potential temperature, which is a thermodynamic variable conservative under all water phase changes. The generalized frontogenesis function is the projection of a new vector,  $Q^*$ , on the quasihorizontal ice-liquid water potential temperature gradient.  $Q^*$  can be seen as the diabatic version of the quasigeostrophic  $Q$ -vector. In regions of large latent heat release due to phase change, the generalized frontogenesis function,  $F^*$ , is a more complete and precise tool for delimiting upward air flow in frontal zones than the classical quasigeostrophic frontogenesis function. The proposed quasigeostrophic frontogenesis function is tested on a real meteorological situation characterized by the genesis and development of a warm front over northern Iberian Peninsula. The new quasigeostrophic frontogenesis function is compared with the classical Pettersen's function obtaining an improvement not only in the diagnosis of frontal development but also in the location of frontal zones.

## 1. Introduction

A frontogenesis function is a tool of atmospheric dynamic diagnosis. It was defined by Petterssen (1936) as the temporal rate of change along a parcel trajectory of the magnitude of the horizontal potential temperature gradient

$$F = \frac{d}{dt} |\nabla\theta| \quad (1)$$

This function is related, in the special case of horizontal flow, to the horizontal divergence and the resultant deformation which are kinematic quantities that are invariant under coordinate transformations. Important dynamic insights into frontogenesis have been developed by quasigeostrophic balance assumptions. Hoskins *et al.* (1978) showed that the Q-vector in horizontal adiabatic quasi-geostrophic flow is the temporal rate of change of the vector potential temperature gradient along a trajectory defined by the geostrophic flow

$$Q = \frac{d_g}{dt} \nabla_p \theta \quad (2)$$

where the subscript  $g$  denotes geostrophic and  $p$  represents differentiation on a constant pressure surface. Hoskins and Pedder (1980) defined the quasigeostrophic frontogenesis function in terms of the Q-vector as

$$F = \frac{\nabla_p \theta}{|\nabla_p \theta|} \cdot Q \quad (3)$$

in which the contribution of the ageostrophic flow is neglected in defining parcel trajectory. Frontogenesis is indicated by zones where the Q-vectors and the temperature gradient are pointing in the same direction. The direction of the Q-vector shows the manner in which temperature gradients are tending to change moving with the fluid. Since the Q-vector is derived under adiabatic conditions, only broad aspects of the vertical motion or frontogenesis patterns can be obtained because small zones of maximum vertical motion or frontogenesis (responsible for maximum precipitation) are associated with zones of latent heat release. In agreement with Hoskins and Pedder (1980), we think that the absence of diabatic processes in quasigeostrophic diagnosis might be a drawback. The purpose of this paper is thus to remedy this situation by incorporating diabatic effects related to changes of water phases into the Q-vector and proposing a generalization of the classic frontogenesis function in order to improve the diagnosis and prediction of frontal zones.

## 2. Generalized frontogenesis function

A frontal zone is defined as a zone of strong gradients of variables such as density, temperature or dry potential temperature. Usually, the dry potential temperature of individual air parcels has been used in the definition of the frontogenesis function since it is conserved under adiabatic conditions. When the effects of heat release due to cloud condensation are taken into account, the dry potential temperature is not an appropriate parameter because it is not conservative, and it does not represent the individual air parcels. If an air parcel containing dry air, water vapor, liquid water and ice is considered, then the ice-liquid water potential temperature  $\theta_{il}$  defined by Tripoli and Cotton (1981) would be more suitable to characterize the system and hence to define the frontogenesis function. This variable has been used to consider diabatic effects on synoptic scale processes (Martín *et al.*, 1997). Tripoli and Cotton (1981) based the definition of  $\theta_{il}$  on an approximated form of the thermodynamic energy equation and made some further approximations to obtain the following expression

$$\theta_{il} = \theta \left[ 1 - \frac{L_{lv}(T_o)r_l}{C_p \max(T, 253)} - \frac{L_{iv}(T_o)r_i}{C_p \max(T, 253)} \right] \quad (4)$$

where  $L_{iv}$  is the latent heat of sublimation,  $L_{lv}$  the latent heat of vaporization,  $r_i$  the mixing ratio of ice water,  $r_l$  the mixing ratio of liquid water, and  $C_p$  is the specific heat of dry air at constant pressure.

This variable is conserved under all phase changes of water if reversibility is assumed (i.e. for non precipitating systems) varying continuously from clear air to cloudy air and it reduces to  $\theta$  in subsaturated conditions. Because it is often desirable to handle a thermodynamic variable which is conservative under adiabatic liquid and ice transformations, the variable  $\theta_{il}$  was defined by Tripoli and Cotton (1981) so that its internal variations are zero. External variations in  $\theta_{il}$  occur only due to external changes of  $r_l$  and  $r_i$ . The representation of a realistic thermodynamic system of cloudy air in terms of the conserved thermal variable  $\theta_{il}$  is more accurate than the system characterization in terms of the dry potential temperature. Hence,  $\theta_{il}$  is more efficient in characterizing the air masses related to frontal zones.

Including  $\theta_{il}$  in Petterssen's (1936) frontogenetical function, eq. (1), a generalized frontogenesis function,  $F^*$ , can be defined in the form

$$F^* = \frac{d}{dt} |\nabla_p \theta_{il}| = \frac{\nabla_p \theta_{il}}{|\nabla_p \theta_{il}|} \cdot \frac{d}{dt} \nabla_p \theta_{il} \quad (5)$$

Assuming quasigeostrophic flow and after rearrangement, the generalized frontogenesis function may be rewritten as

$$F^* = \frac{\nabla_p \theta_{il}}{|\nabla_p \theta_{il}|} \cdot \left[ \nabla_p \frac{d_g \theta_{il}}{dt} - \nabla_p \mathbf{V}_g \nabla_p \theta_{il} \right] \quad (6)$$

If reversibility is assumed,  $d_g \theta_{il}/dt = 0$  and  $\theta_{il}$  remains constant for any parcel of cloudy air, it follows that

$$F^* = \frac{\nabla_p \theta_{il}}{|\nabla_p \theta_{il}|} \cdot [-\nabla_p \mathbf{V}_g \nabla_p \theta_{il}] \quad (7)$$

It can be noted that this generalized frontogenesis function is the projection of a new vector on the quasihorizontal ice-liquid water potential temperature gradient being this new vector

$$\mathbf{Q}^* = \left[ -\frac{\partial \mathbf{V}_g}{\partial x} \cdot \nabla_p \theta_{il}, -\frac{\partial \mathbf{V}_g}{\partial y} \cdot \nabla_p \theta_{il} \right] \quad (8)$$

$\mathbf{Q}^*$  represents the rate of change of the horizontal ice-liquid water potential temperature gradient across an air parcel due to horizontal velocity gradients, i.e., due to parcel rotation and deformation. The  $\mathbf{Q}$ -vector is the adiabatic version of the generalized  $\mathbf{Q}^*$ -vector. In absence of condensate phases, for a dry system,  $\mathbf{Q}^*$  reduces to  $\mathbf{Q}$ . Thus, the final expression for the generalized frontogenesis function can be written as

$$F^* = \frac{\nabla_p \theta_{il}}{|\nabla_p \theta_{il}|} \cdot \mathbf{Q}^* \quad (9)$$

The generalized frontogenesis function is the projection of  $\mathbf{Q}^*$  onto the  $\theta_{il}$  gradient. It displays the manner in which  $\theta_{il}$  gradients are tending to change moving with the fluid, indicating regions where the  $\theta_{il}$  gradients are being enhanced. In regions of large latent heat release due to phase changes, the  $F^*$  could be more successful in delimiting the frontogenetical zones than  $F$  is.

For understanding and application, a rectangular Cartesian coordinate system is taken with the x-axis parallel to the  $\theta$  and  $\theta_{il}$  contours and the y-axis towards colder air. In this reference system, changes in  $\theta$  and  $\theta_{il}$  along the x-axis vanish and the Q- and Q\*-vectors are expressed by

$$Q = \left[ -\frac{\partial v_g}{\partial x} \frac{\partial \theta}{\partial y}, -\frac{\partial v_g}{\partial y} \frac{\partial \theta_{il}}{\partial y} \right] \quad (10a)$$

$$Q^* = \left[ -\frac{\partial v_g}{\partial x} \frac{\partial \theta_{il}}{\partial y}, -\frac{\partial v_g}{\partial y} \frac{\partial \theta_{il}}{\partial y} \right] \quad (10b)$$

where  $v_g$  is the y-component of the geostrophic wind. In this framework, the components of the Q- and Q\*-vectors are related to the horizontal shear and the confluence of the geostrophic wind. In Figure 1 these motions are displayed in order to see the direction of the vectors. For horizontal shear (Fig. 1a),  $v_g$  is an increasing function of  $x$  and, by eq (10), Q and Q\* are pointing towards the area where the air flows from warm to cold zone. For confluence (Fig. 1b),  $v_g$  is a decreasing function of  $y$  with Q and Q\* pointing towards the warm area. Therefore, horizontal shear contributes to change the direction of the temperature

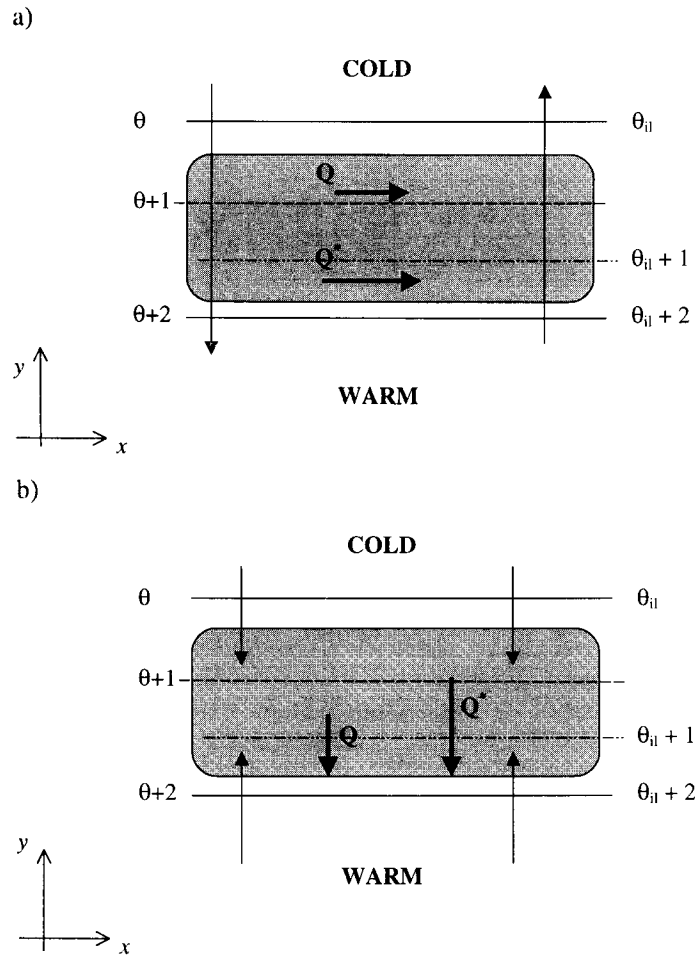


Fig. 1. A possible horizontal section showing  $\theta$  (dashed line) and  $\theta_{il}$  (dotted line) contours. Solid lines indicate isotherms in which  $\theta$  and  $\theta_{il}$  values are equal. The shaded part represents an idealized cloudy area. Geostrophic wind (light arrows) and Q- and Q\*-vectors (heavy arrows) are displayed for: (a) horizontal shear and (b) confluence of the geostrophic wind.

gradients by rotating the isotherms while confluence modifies their magnitudes by stretching. Although both  $Q$ - and  $Q^*$ - vectors indicate upward motion of warm air, the main difference between them is the magnitude. As Hoskins *et al.* (1978), the  $Q$ -vector is proportional to the geostrophic wind gradient

$$Q \propto \frac{1}{L_\theta} \nabla v_g \quad (11)$$

where  $L_\theta$  denotes the separation between  $\theta$ s successive contours. In the same way, the  $Q^*$ - vector could be considered as

$$Q^* \propto \frac{1}{L_{\theta_{ii}}} \nabla v_g \quad (12)$$

where  $L_{\theta_{ii}}$  is the separation of  $\theta_{ii}$  contours. Since  $\theta_{ii}$  decreases in presence of ice and/or liquid water,  $L_{\theta_{ii}}$  distance between  $\theta_{ii} + 2$  (solid) and  $\theta_{ii} + 1$  (dotted) lines will be lesser than the  $L_\theta$  distance between  $\theta + 2$  (solid) and  $\theta + 1$  (dashed) lines in the warm side. As a result the  $Q^*$ - vector will contribute to a higher isotherm rotating and stretching than the  $Q$ - vector does, and so it will show more clearly the frontogenesis effects. Therefore, the generalized quasigeostrophic function,  $F^*$ , in terms of the  $Q^*$ - vector may become a more complete and precise tool for delimiting rising warm air in the frontal zones.

### 3. A case example: the meteorological event of 15-17 October 1990

The proposed quasigeostrophic frontogenesis function is tested on a meteorological situation which is characterized by the genesis of a warm front over northern Iberian Peninsula quickly developing and advancing towards Ireland and Britain Islands. The new quasigeostrophic frontogenesis function is compared with the classical Pettersen's (1936) function in order to examine the possible improvement in the diagnosis of frontal development.

The gridded analyses used to calculate the meteorological fields for 15-17 October 1990 come from the numerical weather prediction limited area model of the Spanish Meteorological Center (Díaz-Pabon, 1988). These analyses are available at all mandatory levels from 1000 to 100 hPa every 12 hours and have a horizontal resolution of  $0.91^\circ \times 0.91^\circ$  latitude-longitude.

On 15 October, an upper trough slowly moving towards Iberia and a zone of strong temperature gradient in the lower troposphere over Iberia can be observed (Fig. 2a). While this temperature gradient is initially dynamically inactive, there is a moderately active cold front associated with the upper trough. The upper flow over Iberia promotes cyclonic curvature causing limited dynamical ascent as it can be observed in the divergence of  $Q$ -vector (Fig. 2b) and greater values in the divergence of  $Q^*$ -vector (Fig. 2c). There is surface pressure fall over Iberia developing warm air advection within the temperature gradient zone. At the same time, there is cold air advection in the western coastal zone so that a strong gradient in thermal advection is created over Iberia. In fact, on 16 October (Fig. 3a), a thermal ridge over Iberia is arising. In these conditions, there must be ascending air ahead and descending air to the rear of the thermal ridge. This situation can be clearly observed in the divergence of  $Q^*$ -vector (Fig. 3c) while the divergence of  $Q$ -vector only indicates ascending air in western Iberia (Fig. 3b). At this point, it must be highlighted the existence of a warm air advection zone over Britain (Fig. 3a) that it is not associated with any significant ascent because there is not cyclonic vorticity advection aloft. On the next day (Fig. 4a), the upper trough axis is situated over Iberia while an upper ridge can be observed over Britain. There are warm air and positive vorticity advections over the rear of the upper ridge axis, both of them contribute to ascent over south Britain. This situation is noticeable in the  $Q^*$ -vector divergence field (Fig. 4c) while the  $Q$ -vector field (Fig. 4b) does not exhibit any significant value over that area.



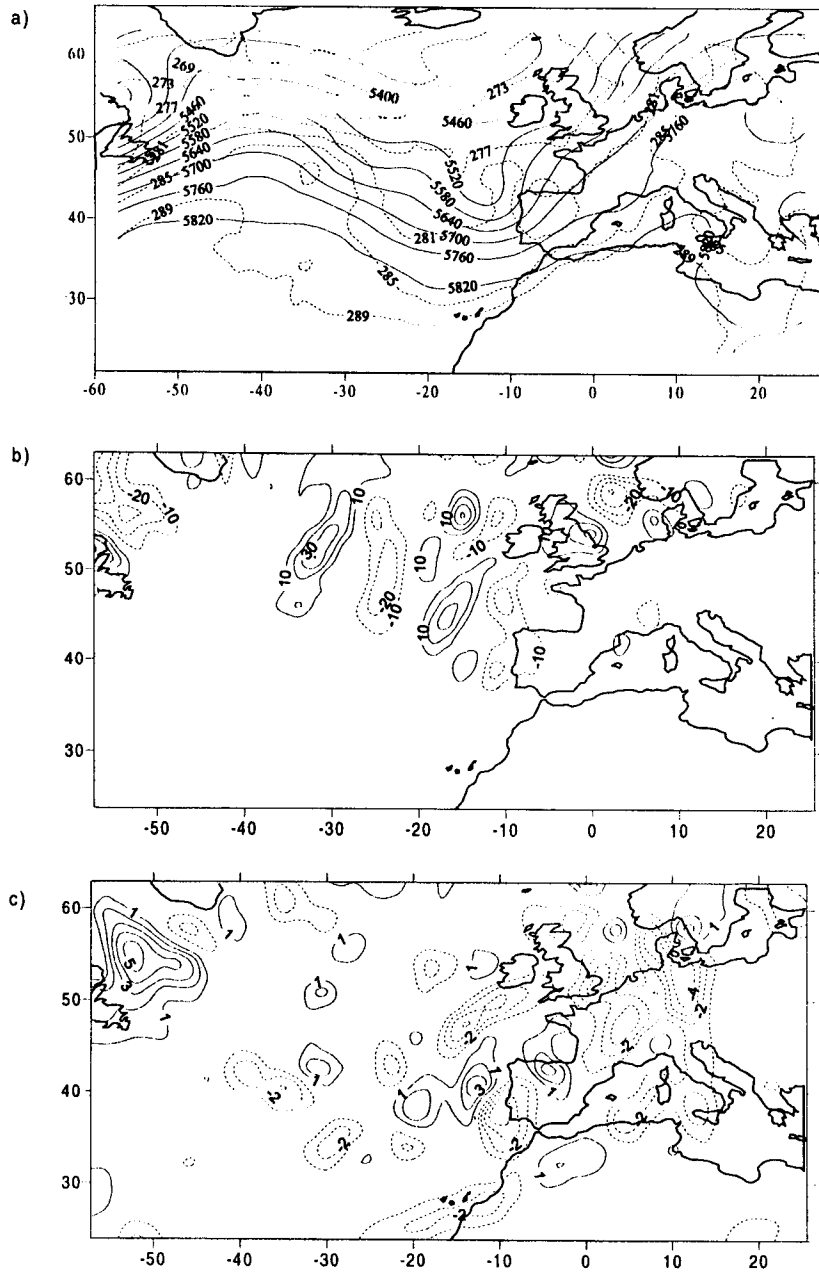


Fig. 3. Same as Fig. 2 except for 16 October 1990.

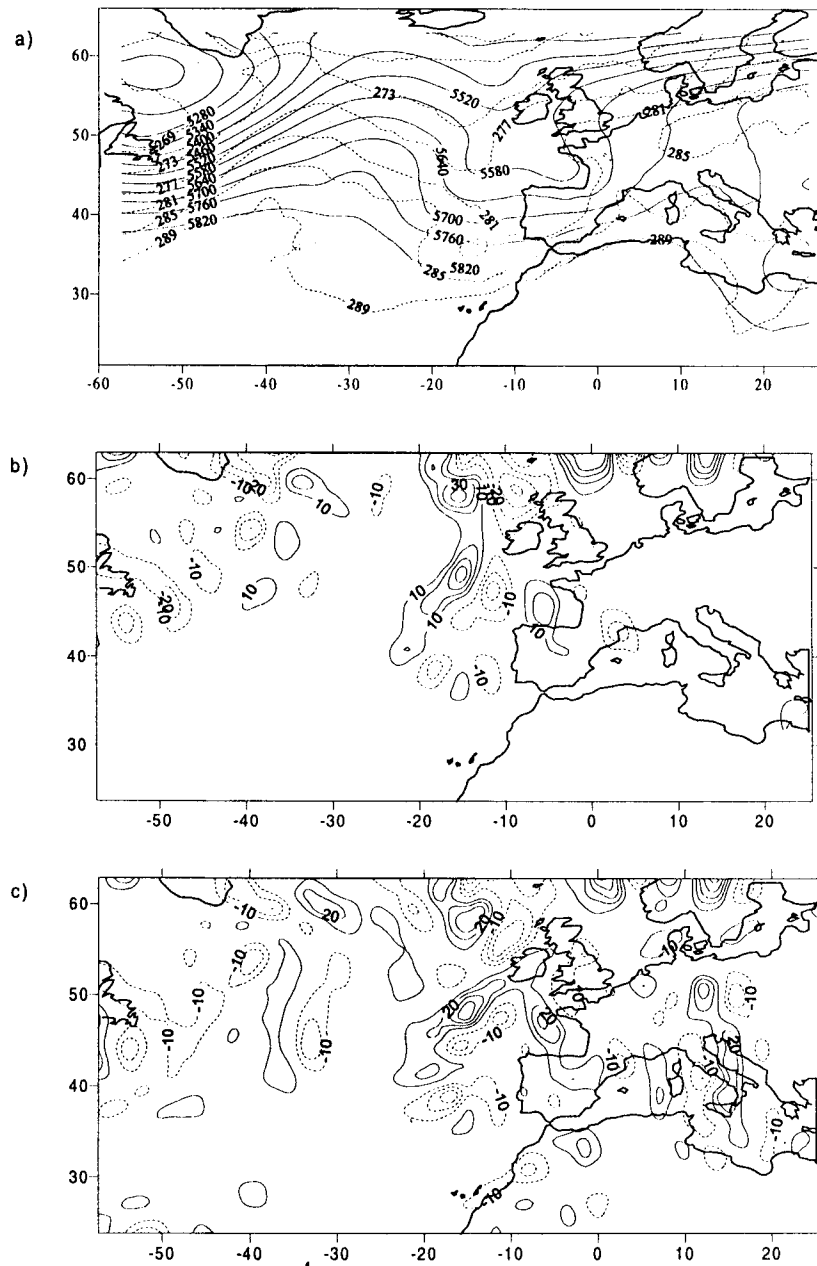


Fig. 4. Same as Fig. 2 except for 17 October 1990.



Throughout the total event, the initial cold front associated with the upper trough tends to lose its identity whereas the dynamically inactive temperature gradient zone over Iberia becomes the main frontal zone quickly advancing towards Ireland and Britain Islands as it can be observed in the sequence of satellite images in Figure 5. These characteristics are clearly noticeably observed in the generalized frontogenesis function,  $F^*$  (Fig. 6). This generalized frontogenesis function, defined in terms of the ice-liquid water potential temperature, is able to identify both frontolitical and frontogenetical processes. It can be noted how  $F^*$  fields at 700 hPa exhibit values of  $-8 \cdot 10^{-10} \text{ K m}^{-1} \text{ s}^{-1}$  and  $8 \cdot 10^{-10} \text{ K m}^{-1} \text{ s}^{-1}$ , respectively, while the classic frontogenesis function fields clearly underestimate the frontogenetical tendency in the whole event as can be observed in Figure 7 where it does not appear any significant value except for a small frontolitical area over southwestern Iberia. Therefore, the new frontogenesis function is able to reproduce the formation and evolution of the fronts recognizing both frontolitical process that occurs in the original cold front and the frontogenetical one that leads to developing the new frontal zone over the northern Iberia.

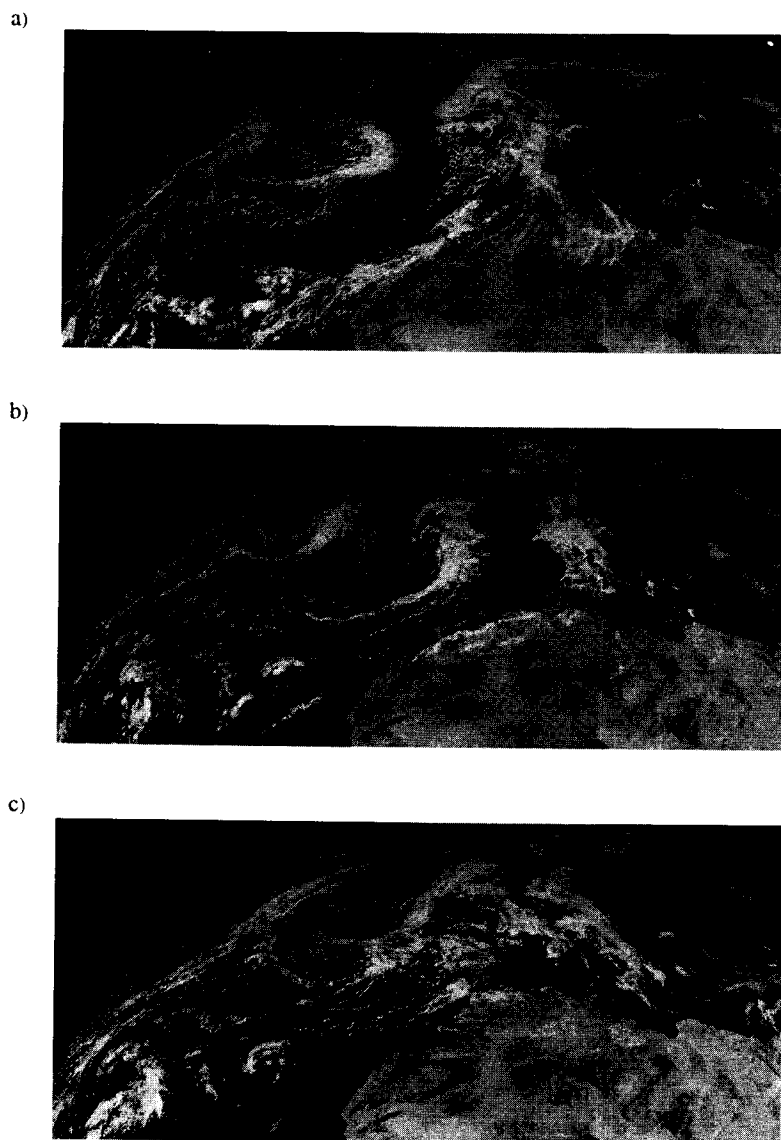


Fig. 5. Meteosat (©2000 EUMETSAT) visible images for the event: (a)-(c) 15-17 October 1990 at 1200 GMT.

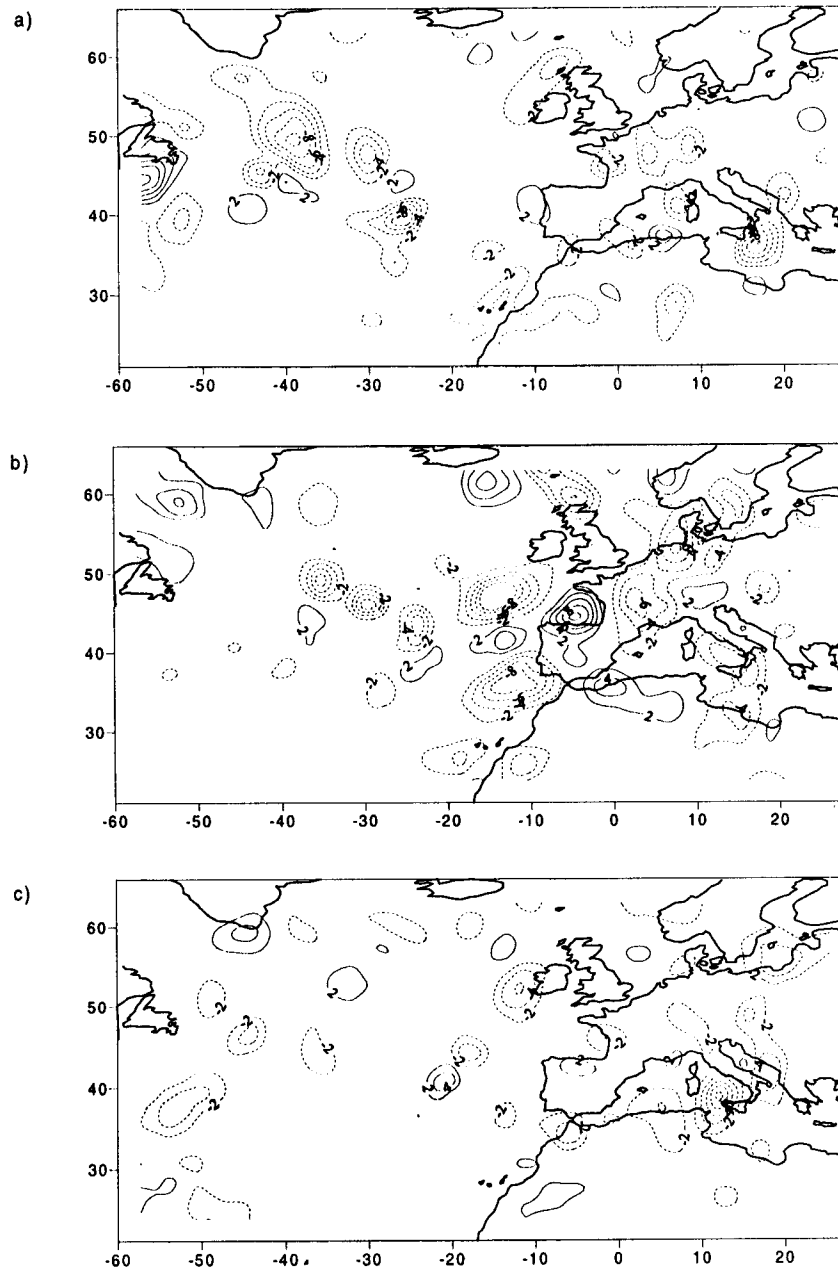


Fig. 6. Generalized frontogenesis function at 700 hPa for: (a)-(c) 15-17 October 1990 at 1200 GMT. Solid (dashed) lines indicate frontogenesis (frontolysis). The contours are in  $10^{-10} \text{ K m}^{-1} \text{ s}^{-1}$ .

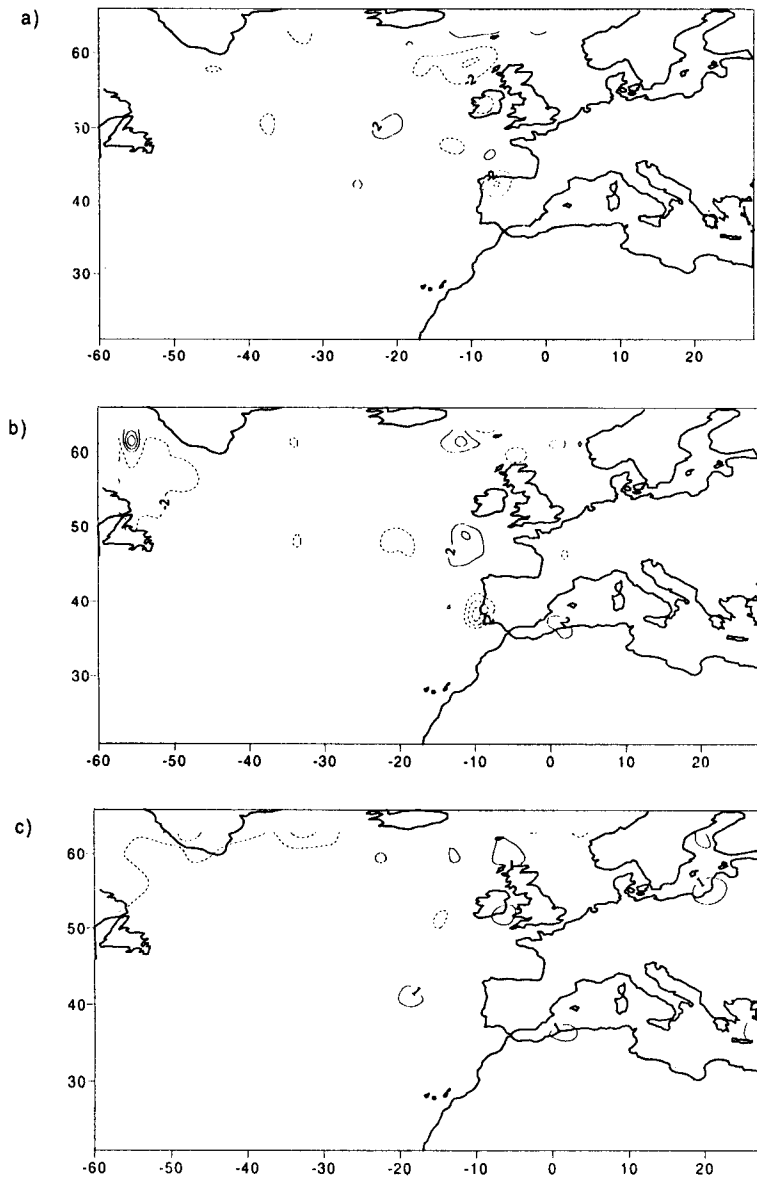


Fig. 7. Same as Fig. 6 except for the classical frontogenesis function.

#### 4. Concluding remarks

This paper is focused on the proposition of a generalized quasigeostrophic frontogenesis function, defined in terms of the ice-liquid water potential temperature. The skillful of this new frontogenetical function is tested on a real meteorological event. The structure of the fronts is examined from the beginning, during

their intensification and in the mature stages by means of several meteorological fields as well as the classic and the generalized frontogenesis functions. Location of the vertical motion areas has been improved by including diabatic effects related with water phase changes into the  $Q^*$ - vector.

While the frontolitical and frontogenetical processes have been well described from the  $F^*$  fields by diagnosing both frontal development and evolution, the classic frontogenesis function does not successfully reproduce any of these features. The improvement in the diagnosis of frontal tendency is due to inclusion of the moist effects by means of the ice-liquid water potential temperature in the definition of  $F^*$ .

### Acknowledgments

The authors wish to thank the Spanish Meteorological Center (Instituto Nacional de Meteorología) and the European Organisation for the Exploitation of Meteorological Satellites (©2000 EUMETSAT) for facilitating the satellite images. They would also like to acknowledge the enthusiastic support and encouragement of Dr. García-Miguel and his valuable comments.

### REFERENCES

- Díaz-Pabon, R., 1988. Modelo operativo en el I. N. M. de análisis numérico tridimensional de campos meteorológicos. Ed. Instituto Nacional de Meteorología, Pub. A-135.
- Hoskins, B. J., I. Draghici and H. C. Davies, 1978. A new look at the  $\omega$ -equation. *Quart. J. R. Met Soc.*, **104**, 31-38.
- Hoskins, B. J., and M. A. Pedder, 1980. The diagnosis of middle latitude synoptic development. *Quart. J. R. Met Soc.*, **106**, 707-719.
- Martín, M. L., M. Y. Luna and F. Valero, 1997. Evidence for the role of the diabatic heating in synoptic scale processes. *Ann. Geophysicae*, **15**, 487-493.
- Petterssen, S., 1936. A contribution to the theory of frontogenesis. *Geofys. Pub.*, **11**, 1-27.
- Tripoli G. J. and W. R. Cotton, 1981. The use of ice-liquid potential temperature as a thermodynamic variable in deep atmospheric models, *Mon. Wea. Rev.*, **109**, 1094-1102.